Int J Adv Manuf Technol (2010) 49:485–495
DOI 10.1007/s00170-009-2433-9

ORIGINAL ARTICLE

Response of materials as a function of grinding angle on friction and transfer layer formation

Pradeep L. Menezes · Kishore · Satish Vasu Kailas · Michael R. Lovell

Received: 17 March 2009 / Accepted: 9 November 2009 / Published online: 26 November 2009

Abstract Surface texture influences friction and transfer layer formation during sliding contact. In the present investigation, basic studies were conducted using an inclined pin-on-plate sliding apparatus to understand the effect of grinding mark directionality on the coefficient of friction and transfer layer formation. In the experiments, 080 M40 steel plates were ground to attain different surface roughness with unidirectional grinding marks. Pins consisting of soft materials (pure Al, pure Mg, and Al–4Mg alloy) were then slid against the prepared steel plates. The grinding angle (angle between direction of sliding and grinding marks) was varied between 0° and 90° in the tests. The experiments were conducted under both dry and lubricated conditions in an ambient environment. It was observed that the transfer layer formation and the coefficient of friction depend primarily on the directionality of the plate grinding marks. For the case of pure Mg pins, a stick-slip friction phenomenon was observed for all grinding angles under dry conditions and for grinding angles over 25° under lubricated conditions. In the case of Al pins, the stick-slip phenomenon was observed only under lubricated conditions for angles exceeding 25°. The stick-slip phenomena did not occur in any of the conditions studied with Al–4Mg alloy pins. Based on the results, it was concluded that the magnitudes of the friction and the stick-slip motion amplitude (for Al and Mg pins) were primarily controlled by changes in the level of plowing friction.

Keywords Friction · Transfer layer · Stick-slip · Surface texture · Surface roughness

P. L. Menezes · Kishore
Department of Materials Engineering, Indian Institute of Science, Bangalore 560 012, India

S. V. Kailas (✉)
Department of Mechanical Engineering,
Indian Institute of Science,
Bangalore 560 012, India
e-mail: satvk@mecheng.iisc.ernet.in

M. R. Lovell
Department of Industrial Engineering,
University of Wisconsin-Milwaukee,
Milwaukee, WI 53201, USA

Present Address:
P. L. Menezes
Department of Industrial Engineering,
University of Wisconsin-Milwaukee,
Milwaukee, WI 53201, USA

1 Introduction

Friction, the resistance to relative motion of two bodies that are in contact, is a subject that has been of interest to mankind for ages. It is described in terms of a coefficient that is defined as the ratio of the tangential force to the normal force. The important factors that control friction are affected by (1) kinematics of the surfaces in contact (i.e., the direction and the magnitude of the relative motion between the surfaces in contact), (2) externally applied load and/or displacements, (3) environmental conditions such as temperature and lubricants, (4) surface texture, and (5) material properties [1].

Among the various factors which influence friction, the effect of surface texture during the sliding contact of materials with significantly different hardness values is the focus of the present study. Examining the literature, a few authors have accounted for the role of surface texture of softer materials involved in sliding contact [2–5]. The

surface texture of the more deformable material alone, however, cannot fully explain the variations of friction during sliding. It is also important to understand the influence of the surface texture of the harder material because of its impacts on the surface energy. For this purpose, extensive research has been carried out to study the role that surface texture of harder materials has on the friction during sliding [6–12]. Staph et al. [6] studied the effect of surface texture and surface roughness on scuffing using a caterpillar disc tester. In previous work by the authors [6], steel discs of varying roughness and texture were used to determine that both surface texture and surface roughness influence frictional behavior. Määttä et al. [7] studied the friction of stainless steel strips against different tool steels. They concluded that the surface topography of the tool has a marked influence on the friction between the tool and the workpiece. Malayappan and Narayanasamy [8] studied the bulging effect of aluminum solid cylinders and concluded that barreling levels depend on the surface texture of the hardened die surfaces. Lakshmipathy and Sagar [9] examined the effect of die surface texture on interfacial friction and found that the friction was lower for criss-cross surface patterns. Menezes et al. [10–12] studied the effect of surface texture on the friction and transfer layer formation for various materials using an inclined scratch test device. In these works, it was determined that a surface texture that promotes plane strain conditions near the interface yields higher friction and a surface texture that promotes plane stress conditions results in lower values of friction. In the present investigation, the influence of grinding mark direction on the friction and formation of a transfer layer is investigated when a soft pin slides relative to a hardened ground plate. To this end, experiments were conducted using an inclined pin-on-plate sliding apparatus with pure Al, pure Mg and Al–4Mg alloy pins, and hardened steel plates of varying roughness under both dry and lubricated conditions.

1.1 Experimental details

In preparation for the experiments, unidirectional grinding marks with varying roughness were produced on 080 M40 steel plates with emery papers of 220, 400, 600, 800, and 1000 grit sizes. Figure 1 shows the three-dimensional surface profiles of an as-ground steel plate with unidirectional grinding marks (produced with 600 grit emery paper). The three-dimensional profiles were obtained for a scan size of 2.4 mm×1.8 mm using an optical profilometer. The resolutions in the vertical and horizontal direction were found to be 1 nm and 300 nm, respectively. It should be noted that the R_a value indicated in Fig. 1 is the three-dimensional surface roughness, i.e., the average of the entire surface. Overall, the steel plate's dimensions were

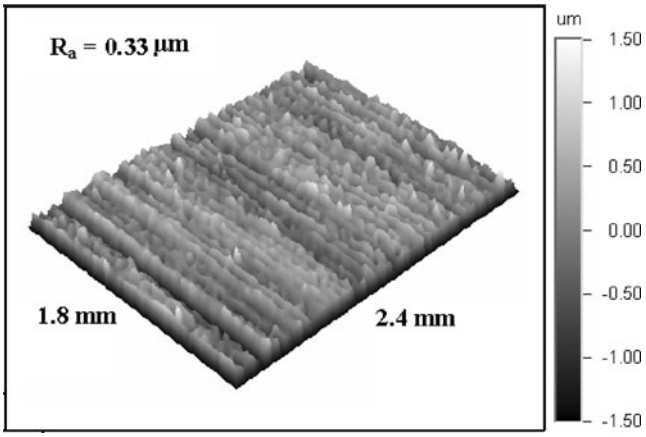

Fig. 1 3D profile of unidirectionally ground steel plate

28 mm×20 mm×10 mm (thickness). Al–4 wt.% Mg alloy, high purity Al (99.997 wt.%), and pure Mg (99.98 wt.%) cylindrical stock were then machined to produce pins that were 10 mm long, 3 mm in diameter, and had a tip radius of 1.5 mm. After machining, the pins were electro-polished to remove any work-hardened layers that might have formed. Hardness measurements of the pins and steel plate were made at room temperature using a Vickers microhardness tester with a 100 g load and 10-s dwell time. Average hardness values obtained from five indentations were found to be $105HV_{0.1}$, $31HV_{0.1}$, and $55HV_{0.1}$ for the Al–4Mg alloy, high purity Al, and pure Mg pins, respectively; the hardness of the steel plate was found to be $205HV_{0.1}$. Before each experiment, the pins and steel plates were thoroughly rinsed with an aqueous soap solution. This was followed by cleaning the pins and plates with acetone in an ultrasonic cleaner.

The experiments were conducted using the inclined pin-on-plate sliding apparatus schematically depicted in Fig. 2. The stiffness of the pin-on-plate sliding apparatus was found to be 0.16 µm/N. The details of the operation of the apparatus have been presented previously [12]. The advantage of this apparatus is that, from a single experiment, the effect of normal load (up to the test limit of 120 N) on the coefficient of friction could be studied. To perform an experiment, the steel plate was fixed horizontally in the vice of the pin-on-plate sliding tester. The vice setup was then tilted so that the surface of the plate made contact at angular increments of 1±0.1° with respect to the horizontal base. Then, pins were slid at a speed of 2 mm/s against the prepared steel plate starting from the lower end to the higher end of the inclined surface for a sliding length of 10 mm. The normal load was varied from 1 to 120 N during the tests. The normal and tangential forces were continuously monitored using a computerized data acquisition system. The coefficient of friction, μ, which is the ratio of the traction force (T) to the normal force (N), was

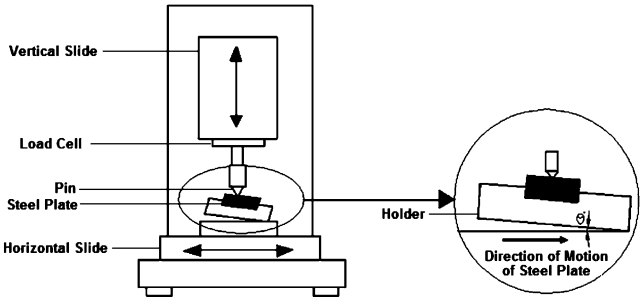

Fig. 2 Schematic diagram of pin-on-plate sliding tester

calculated from the recorded forces using the following formula [12]:

$$\mu = \frac{T}{N} = \frac{F_T \cos\theta - F_N \sin\theta}{F_T \sin\theta + F_N \cos\theta}. \quad (1)$$

In Eq. (1), θ is the angle of inclination of the steel plate, F_T is the recorded traction force, and F_N is the recorded normal force at any instance. The pins were slid at angles of 0° (parallel), 5°, 10°, 15°, 20°, 25°, 45°, 65°, 80°, 85°, and 90° (perpendicular) to the unidirectional grinding marks on the steel plate. Figure 3 schematically represents the steel plate surface with unidirectional grinding marks for three of the 11 angles investigated. Experiments were conducted under both dry and lubricated conditions on each plate in an ambient environment, i.e., 24 to 28°C, and relative humidity of about 40%. The dry tests were conducted first to avoid any additional cleaning of the steel plates and to exclude variations in roughness.

Dry tests were performed to obtain five parallel wear tracks on the same steel plate. Each wear track was produced by a single sliding event. It was observed that the initial sphere-on-plate contact essentially became a flat-on-plate type contact even before the end of the first wear track. At the same time, it was observed that wear track width varied considerably in the first three tests. For this reason, all the results presented were of the fourth wear track. The fifth wear track was made to confirm the consistency in results. The width of the fourth wear track was found to be ~0.8 mm; this translates to a pressure of more than 200 MPa. It was observed that the coefficient of friction did not vary much for all these five wear tracks. After the dry tests, the pin was removed and a new pin from the same material stock was mounted on the vertical slide to perform lubricated tests. For the lubricated tests, 0.05 ml of commercially available engine oil lubricant (SAE 40, API rating SJ class, "Shell" make two-stroke oil) was applied on the surface of the steel plate. The viscosity of lubricant oil was found to be 40 cSt at 40°C and had the extreme pressure additive zinc dialkyl dithiophosphate (ZDDP). The presence of ZDDP was confirmed using a Fourier transform infrared spectroscopy technique. For a given grinding angle, the tests were conducted for five surface roughnesses obtained using the various grit size emery papers. The profiles and surface roughness parameters of the steel plates were measured in the direction of sliding on the bare surface (away from the wear tracks) using an optical profilometer. The average surface roughness, R_a, values for all surfaces are presented in Table 1. As demonstrated by the table, the surface roughness values for different grinding directions were comparable with each other when they were ground against the same grinding media. After the tests, the pins and steel plates were observed using a scanning electron microscope to study the morphology of the transfer layer.

2 Results and discussion

2.1 Variation on friction coefficient

In the present investigation, experiments were performed to obtain the responses of Al–4Mg alloy, pure Mg, and high purity Al as a function of grinding angle. In all the cases examined, it was observed that the coefficient of friction did not vary significantly for normal loads of up to 120 N. Figure 4 shows the variation of coefficient of friction with sliding distance when Al–4Mg alloy pins slid against steel plates at grinding angles of 0°, 20°, 45°, and 90° under both dry and lubricated conditions. In the figure, it is found that the coefficient of friction does not vary significantly with sliding distance. Likewise, for a given grinding angle, the friction did not vary significantly with surface roughness. It was observed, however, that the average coefficient of friction increases considerably with the grinding angle under both dry and lubricated conditions.

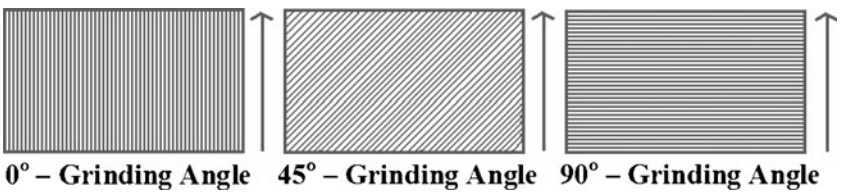

Fig. 3 Schematic diagram of steel plate surface with unidirectional grinding marks. *Arrow* indicates the sliding direction of the pin which makes an angle 0°, 45°, and 90° to the unidirectional grinding marks during sliding

Table 1 Surface roughness values of the plates for different grinding angles and materials

Grinding angle	Emery paper grit size	Surface roughness (R_a, μm) of the steel plate		
		Al–4Mg	Al	Mg
0°	220	0.37	0.34	0.28
	400	0.19	0.25	0.24
	600	0.17	0.21	0.19
	800	0.15	0.20	0.17
	1000	0.14	0.18	0.15
5°	220	0.36	0.25	0.28
	400	0.23	0.23	0.25
	600	0.2	0.22	0.21
	800	0.18	0.2	0.18
	1000	0.17	0.17	0.17
10°	220	0.51	0.39	0.35
	400	0.23	0.28	0.3
	600	0.22	0.23	0.25
	800	0.21	0.22	0.23
	1000	0.2	0.2	0.21
15°	220	0.43	0.36	0.36
	400	0.28	0.34	0.27
	600	0.22	0.31	0.25
	800	0.21	0.24	0.21
	1000	0.19	0.2	0.2
20°	220	0.75	0.42	0.52
	400	0.28	0.32	0.38
	600	0.24	0.31	0.32
	800	0.23	0.27	0.27
	1000	0.21	0.22	0.22
25°	220	0.69	0.42	0.51
	400	0.31	0.37	0.29
	600	0.26	0.33	0.28
	800	0.24	0.27	0.23
	1000	0.23	0.22	0.21
45°	220	0.94	0.69	0.48
	400	0.35	0.34	0.39
	600	0.26	0.22	0.36
	800	0.25	0.21	0.27
	1000	0.24	0.20	0.19
65°	220	0.96	0.78	0.51
	400	0.37	0.5	0.36
	600	0.33	0.35	0.35
	800	0.25	0.23	0.26
	1000	0.22	0.21	0.25
80°	220	0.77	0.52	0.73
	400	0.3	0.4	0.54
	600	0.29	0.27	0.34
	800	0.28	0.26	0.26
	1000	0.22	0.23	0.23
85°	220	0.77	0.7	0.75
	400	0.29	0.5	0.51

Table 1 (continued)

Grinding angle	Emery paper grit size	Surface roughness (R_a, μm) of the steel plate		
		Al–4Mg	Al	Mg
	600	0.26	0.35	0.31
	800	0.23	0.26	0.23
	1000	0.21	0.24	0.21
90°	220	0.73	0.73	0.55
	400	0.42	0.39	0.38
	600	0.26	0.33	0.31
	800	0.24	0.22	0.3
	1000	0.22	0.21	0.29

Figure 5 shows the variation of friction with sliding distance when high purity Al pins were slid against steel plates over a range of grinding angles under both dry and lubricated conditions. Akin to the Al–4Mg alloy, the coefficient of friction increases considerably with grinding angle under lubricated conditions. Under dry conditions, the friction does not vary significantly with grinding angles. In addition, under dry conditions, a stick-slip phenomenon (the oscillation in the coefficient of friction with sliding distance) is not observed for any grinding angles. Under lubricated conditions, however, the stick-slip phenomenon was found at higher loads. Furthermore, it was found that the existence of stick-slip phenomenon and its amplitude depends on the grinding angles where the onset of oscillations occur at grinding angles of 25° and increase in magnitude through 90°.

Figure 6 shows the variation of friction with sliding distance when pure Mg pins were slid against steel plates at different grinding angles under dry and lubricated conditions. Similar to the Al–4Mg alloy, the friction increases considerably as the grinding angle increases under both dry and lubricated conditions. Stick-slip phenomenon was observed for all grinding angles under dry conditions, the amplitude of which increases with grinding angle. Under lubricated conditions, the stick-slip behavior is observed at 25° and increases through 90°.

Figure 7a and b depicts the variation of the average coefficient of friction with grinding angle for Al–4Mg alloy, high purity Al, and pure Mg pins slid on steel plates with varying roughness under both dry and lubricated conditions. The error bars in the figure indicate the maximum and minimum values of the coefficient of friction for each roughness tested. Each symbol on Fig. 7 represents the average coefficient of friction of five roughnesses tested at the same grinding angle. It was observed that the range of surface roughness, R_a, varies between 0.1 and 1.0 μm for different grinding angles. Throughout the experiments, the friction did not vary with R_a at a given grinding angle. In

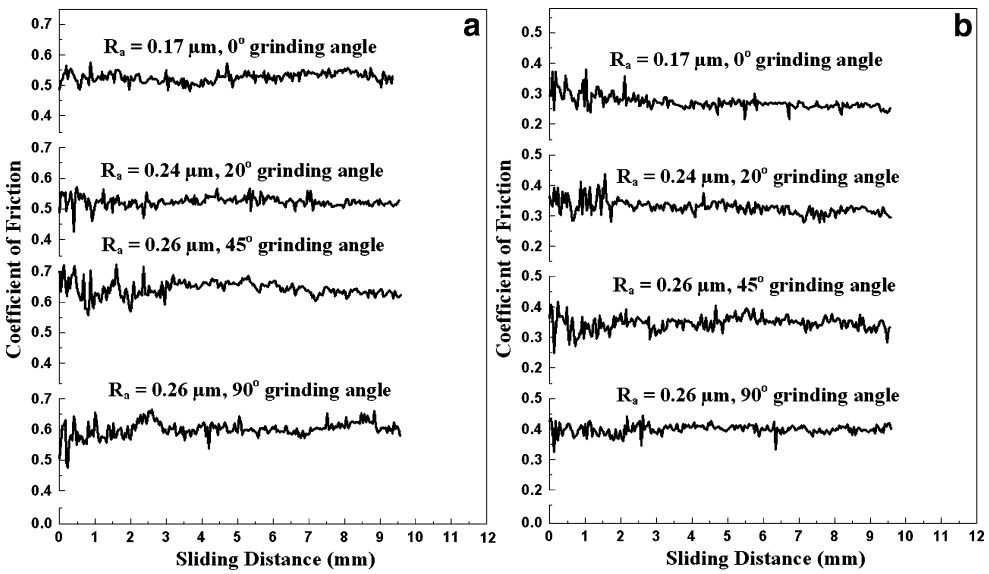

Fig. 4 Variation of coefficient of friction with sliding distance when Al–4Mg alloy pins slide against steel plates at different grinding angles under **a** dry and **b** lubricated conditions

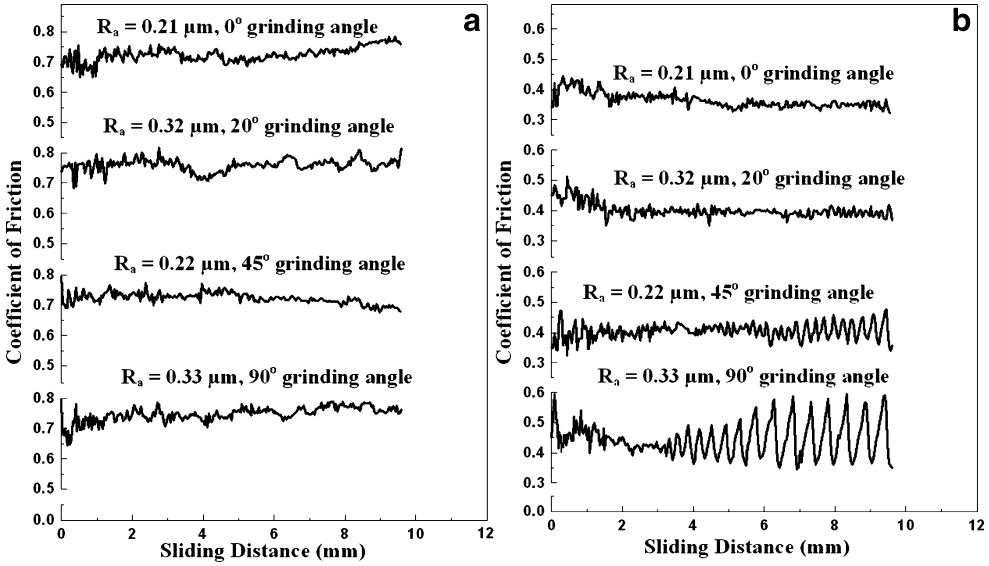

Fig. 5 Variation of coefficient of friction with sliding distance when high purity Al pins slide against steel plates at different grinding angles under **a** dry and **b** lubricated conditions

Fig. 7a and b, it was observed that the coefficient of friction varies considerably with grinding angles under both dry and lubricated conditions. Under lubricated conditions, the friction rapidly increases to an angle of 25° before leveling off.

2.2 Transfer layer results

Figure 8a–d shows backscattered scanning electron micrographs of the steel plate surfaces tested under dry conditions at grinding angles of 0°, 20°, 45°, and 90°. In the figures, a large amount of Al–4Mg alloy transfer layer was found on the steel plate surfaces under dry conditions where direct surface asperity contact occurs. As expected, it was observed that the amount of transfer layer increases as the normal load increases. Similar observations were found at other grinding angles. The figures also indicate that the amount of transfer layer formed on the steel plate was larger under dry conditions than under lubricated conditions (Fig. 8e–h) and that the transfer layer magnitude increases considerably with grinding angle. It was additionally observed at all conditions that the amount of the transferred layer formed on the steel plate did not substantially vary with the surface roughness. Identical trends were found for the case of pure Mg. For the case of high purity Al (under dry conditions), however, the amount of transfer layer formed on the steel plate did not appreciably vary with grinding angles. The reason for such a trend will be discussed in a later section.

Scanning electron micrographs of the Al–4Mg alloy pins tested under dry conditions for all grinding angles showed strong surface shearing and plowing marks on the contacting surface. Under lubricated conditions, the intensity of surface shearing reduced because of the hydrodynamic lift

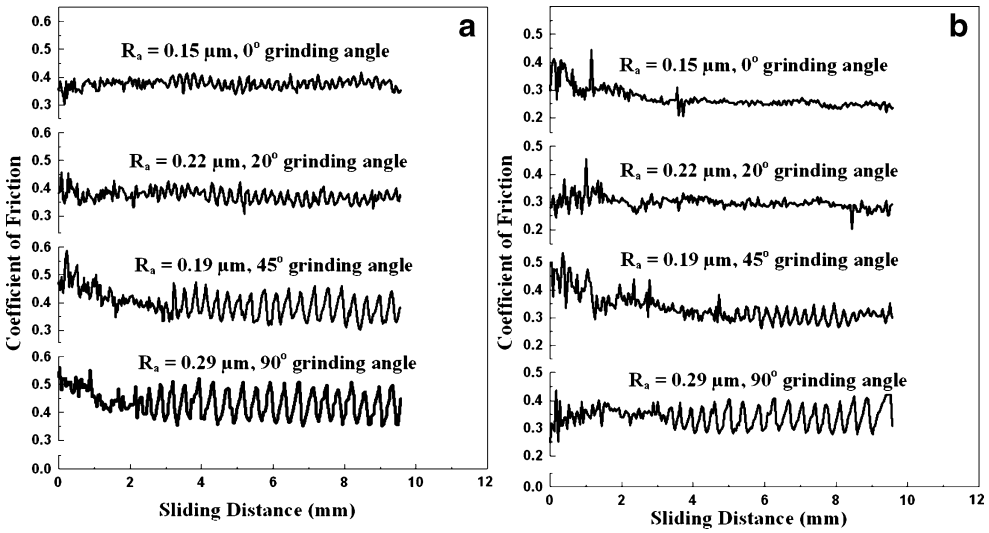

Fig. 6 Variation of coefficient of friction with sliding distance when pure Mg pins slide against steel plates at different grinding angles under **a** dry and **b** lubricated conditions

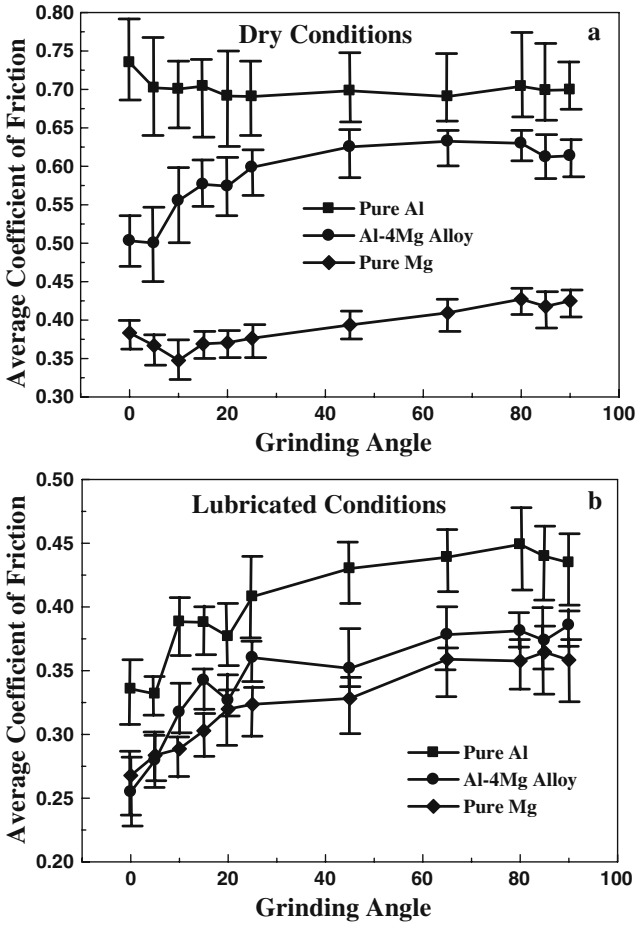

Fig. 7 Variation of friction with grinding angle under **a** dry and **b** lubricated conditions

provided. Similar observations were found for high purity Al and pure Mg. In the case of Al, a small amount of iron transferred from the steel plate to the Al pin surface under dry sliding conditions. It was further observed that the amount of transferred iron (to softer pins) increased as the grinding angle increased. The amount of transferred iron on the pin surface decreased with the application of lubricant because of decreased surface interaction. The amount of transferred iron did not vary with grinding angle under lubricated conditions. For the case of Al and Mg, plowing marks normal to the sliding direction were observed on the pin surface. These plowing marks resulted from the stick-slip phenomenon. For the case of pins sliding at 45° grinding angles, plowing marks formed on the pin surface were at 45° angles to the sliding direction.

2.3 Adhesion and plowing friction analysis

According to Bowden and Tabor [13], the coefficient of friction has two components, namely adhesion and plowing. The adhesion component depends on the material pair, lubrication, and the real area of contact; the plowing component depends on the degree of plastic deformation taking place at the asperity level. The adhesion component of friction can be minimized, if not eliminated, by the introduction of a lubricant at the interface between contacting surfaces. For the conditions tested, the lubrication regime was established using the minimum film thickness equation and the roughness of the mating surfaces [14]. Based on our analysis, it was determined that the coefficient of friction recorded for the lubricated experiments were in the boundary lubrication regime and included plowing components of friction. Figure 9 presents the variation of the components of friction as a function of the testing conditions. In the figure, the adhesive component of friction was determined by taking the difference between the dry and lubricated values at a given operating condition. Examining Fig. 9, it is found that plowing is the dominant friction mechanisms as its value is significantly greater than the adhesive component. Specifically examining the plowing component, Fig. 9 indicates that the plowing friction is lowest for sliding parallel (0° grinding angle) to the unidirectional grinding marks and steadily increases to a perpendicular sliding orientation (90° grinding angle). Because the plowing component is dominant and considerably varies with grinding angle, it can be inferred that the variations in total friction are primarily due to changes in plowing behavior.

Considering the plate surface, the unidirectionally ground surface exhibits a wave-like pattern that is akin to cylindrical ridges (similar to Fig. 1). A schematic of the expected flow pattern for the 90° and 0° grinding angles are shown in Fig. 10a and b, respectively. When the grinding marks are perpendicular to the sliding direction (Fig. 10a), the softer pin material will have to climb over the cylindrical asperities. In this case, there is greater resistance in the direction of sliding, the stresses developed in the plastically deforming material will be large, and the state-of-stress can be characterized as plane strain. Under such conditions, the material can shear ahead of the asperities, leading to higher material transfer. Thus, more of the friction would be characterized by plowing. When the grinding marks are parallel to the sliding direction (Fig. 10b), the pin material experiences less resistance as flow develops along the valleys of the plate asperities. For this condition, the plowing component of friction is lower and the amount of material sheared and transferred is minimized. For other grinding angles (see Fig. 9), the values of the friction and material transfer would fall between these two extremes.

An interesting feature that was observed in the experiments was that the adhesion component of friction remained relatively constant for all materials except Al. The plowing component of friction, in contrast, increases

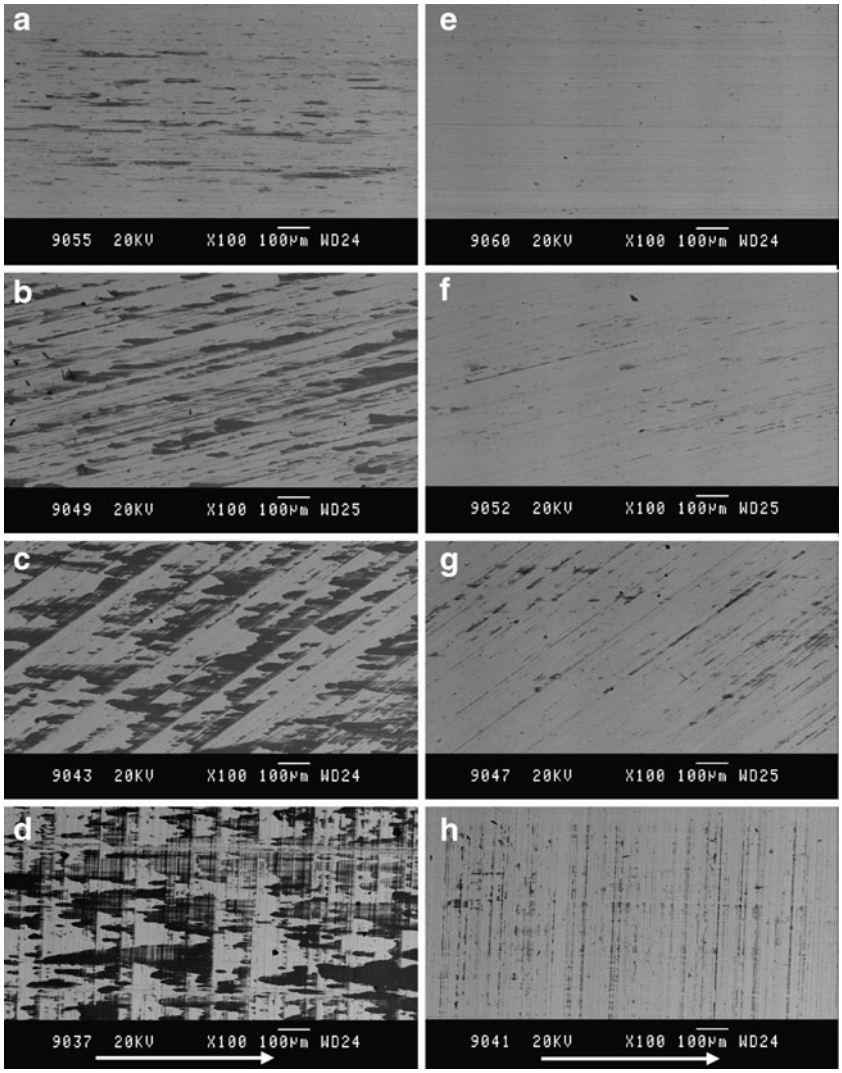

Fig. 8 Backscattered scanning electron micrographs of steel plates when Al–4Mg alloy pins slid at 0° (**a**, **e**), 20° (**b**, **f**), 45° (**c**, **g**), and 90° (**d**, **h**) grinding angles under dry (**a**, **b**, **c**, **d**) and lubricated (**e**, **f**, **g**, **h**) conditions. The *arrows* indicate the direction of the pin movement. The black phase indicates Al–4Mg transfer layer while gray for pure iron

sharply up to a grinding angle of about 25°, after which the rate of change diminishes. Single-asperity interaction by a hard wedge on a soft material, in which the soft material is deformed under plane strain conditions, has been studied by Lovell and Deng [15], Challen and Oxley [16], and Petryk [17]. Using slip line field theory, these works showed that the overall friction coefficient increases when the asperity angle or the interfacial friction increases. In the present set of experiments, the average slope [18, 19] of the surface profile, δa, was measured using a profilometer. Figure 11 shows the variation of δa with grinding angle for different surface roughnesses generated using various emery paper grit sizes. It can be seen that the average slope of the surface profile falls between 1° and 6° for 0° and 90° grinding angles, respectively. The average slope is found to increase monotonically as the grinding angle is increased. The lower slope of the various surfaces indicates that only rubbing models are active [16, 17]. Furthermore, in the present set of experiments, the unidirectional perpendicular tests (grinding angle of 90°) represent a case of single-asperity interaction [15–17]. When the grinding angle is 90°, the resistance to flow is the greatest. As the grinding changes, the resistance to flow becomes a function of the projected asperity area along the sliding direction, which

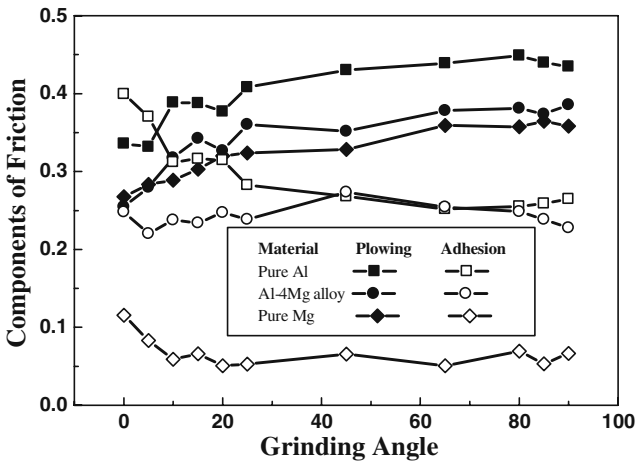

Fig. 9 Variation of components of friction with grinding angle

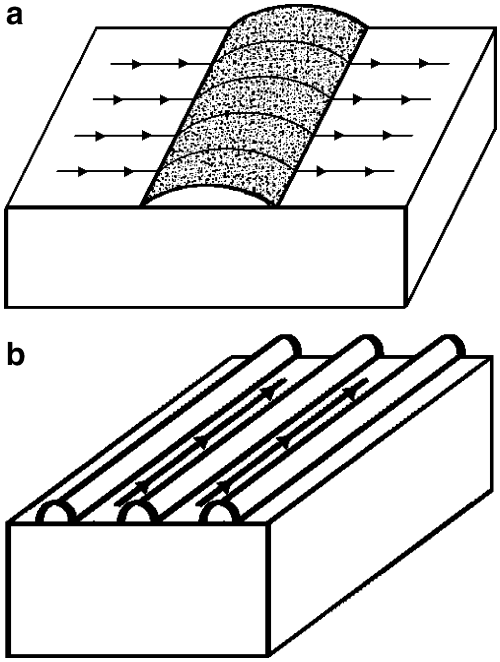

Fig. 10 Schematic diagram of flow pattern for **a** 90° (constrained flow) and **b** 0° (less constrained flow) grinding angles

decreases at lower grinding angles. This projected area would be a function of sin(α), where α is the grinding angle. The rate of reduction of this projected area would then be cos(α). It can be shown that the increase in projected area would be highest when α decreases to zero. The plowing component of friction will then tend to increase more rapidly when the grinding angle is low. This increase is expected to taper off when the grinding angle is high, as observed in Fig. 8 where the plowing component of friction rapidly increases to 25°.

Another interesting finding in the present work relates to the relation between coefficient of friction, μ, and trigonometric grinding angle, $Sin\theta$. The relation between μ and $Sin\theta$, is given by.

$$\frac{\mu_\theta - \mu_0}{\mu_{90} - \mu_0} = Sin\theta \tag{2}$$

In Eq. (2), the values for μ_0=0.26 and μ_{90}=0.39 were determine from Fig. 9 for the case of Al–4Mg alloy. Thus, the theoretical value of μ_θ can be calculated as $\mu_\theta = 0.26 + 0.13(\sin\theta)$. Similar calculations can be made for pure Al $(\mu_0 = 0.34, \mu_{90} = 0.45, \mu_\theta = 0.34 + 0.11(\sin\theta))$ and pure Mg $(\mu_0 = 0.27, \mu_{90} = 0.37, \mu_\theta = 0.27 + 0.10(\sin\theta))$ from Fig. 9. The plot obtained for different values of θ is shown in Fig. 12 for all three materials. The experimental results are also included in the same figure for comparison. Based on Fig. 12, it can be inferred that the plowing component varies as a function of $Sin\theta$.

It was reported earlier for the case of Al that the amount of iron particles transferred to the pin surface reduces as the grinding angle decreases. When pins are slid on the unidirectional ground steel plate, some of the weaker asperities break and adhere to the pin surface. The extent of breaking and transfer of these weaker asperities depend on the grinding angle. The likelihood of plate asperities breaking will increase when aluminum pins are slid perpendicular to the grinding direction. This is because the shear stresses generated when sliding at 90° grinding angle are the highest. Hence, the maximum amount of iron will adhere to the pin surface when the pins are slid perpendicular to the unidirectional grinding marks. From this, it can be inferred that, as the grinding angle increases, the interaction between the aluminum and iron decreases. In

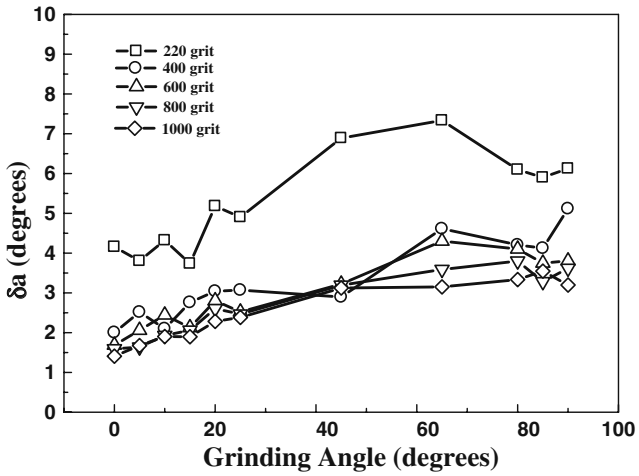

Fig. 11 Variation of average slope of the surface profile, δa, with grinding angle

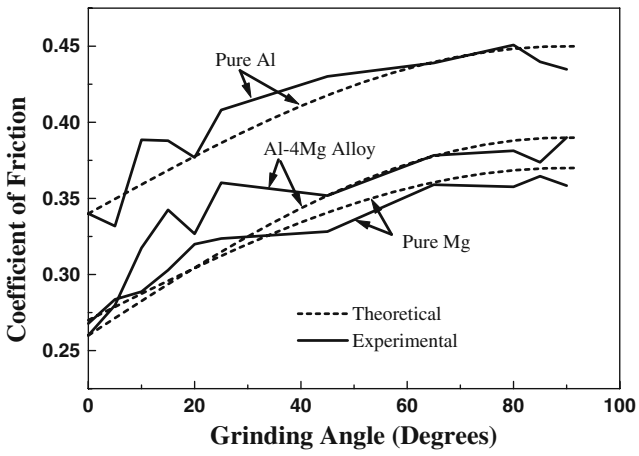

Fig. 12 Variation of theoretical and experimental values of coefficient of friction with grinding angle for case of pure Al, Al–4Mg alloy, and pure Mg

this respect, the interaction between back transferred iron (pin) and iron (plate) increases as the grinding angle increases. It was found previously [13] that the adhesion component depends on material pair. For a given material pair, the adhesion component remains constant under most conditions. In the present experimental conditions, instead of displaying constant adhesion components with grinding angle, it decreases with grinding angle owing to the amount of iron–iron interaction at the asperity level. This fact is reflected in the total coefficient of friction, which remains more or less constant with grinding angle in Fig. 6a.

2.4 Stick-slip motion

It was observed for the case of Al under lubricated conditions that the amplitude of stick-slip oscillations depends on the grinding angle. The amplitude of oscillations starts at 25° and increases through 90°. It can therefore be deduced that the amplitude of stick-slip motion primarily depends on the plowing component (rather than on the adhesion component) of friction. At 90°, the condition at the asperity level is plane strain leading to higher stresses being generated during sliding. The lubricant present at the interface will experience higher compression and increased viscosity. The increased viscosity will ultimately lead to stick-slip motion. As the grinding angle decreases, the degree of plane strain condition decreases, which reduces the amplitude of stick-slip motion.

The existence of stick-slip phenomenon under lubricated conditions has been previously reported [20–22]. Tanaka et al. [20] reported that under high load conditions the lubricant film, confined and sheared between two solid walls, is compressed and solidified which results in stick-slip motion due to molecular deformation. Gee et al. [21] reported that the occurrence of solid-like characteristics are due to the ordering of the liquid molecule into discrete layers. In general, it was concluded [21] that these properties depend not only on the nature of the liquid but also on the atomic structure of the surfaces, the normal pressure, and the direction and velocity of sliding. Demirel and Granick [22] observed liquid-like response at low deformation rates and stick-slip-like response at high deformation rates. In another effort, Ai and Cheng [23] observed maximum film thickness for parallel texture sliding. Based on the literature, the thickness of the lubricant film in the current study is expected to be highest for the 0° grinding angle and lowest for the 90° angle. When the condition of plane strain prevails, the properties of lubricant film are expected to change at higher loads, which lead to stick-slip motion. Thus, the amplitude of oscillation would be the greatest at 90° grinding angles and least for the 0° grinding angle owing to the extent of plane strain conditions. It was observed that the normal load required to initiate stick-slip motion increases at lower grinding angles since higher loads are required to compress the lubricant as the grinding angle decreases. At lower grinding angles, the thickness of the lubricant film is greatest [20], causing the lubricant to behave like a “bulk lubricant” and no stick-slip motion was observed.

Overall, the HCP metals showed different frictional responses when compared to FCC metals under similar testing conditions. For the case of Mg, the stick-stick phenomenon was observed under both dry and lubricated conditions. When comparing the properties of Al and Mg, the two major differences are the hardness and the number of slip systems. Mg has a higher hardness and lower number of slip systems. A lower number of slip systems could itself promote stick-slip motion as some of the grains in contact at the asperity level would be difficult or easy depending on the orientation of the slip planes [24, 25]. Such a difference in slip within the contact zone would promote stick-slip which could explain why stick-slip is observed under both dry and lubricated conditions for Mg. The higher hardness for Mg also reduces the real area of contact of the contacting asperities. This would lead to a lower compression of the lubricant during sliding. When the grinding angle decreases, the extent of interlocking is also expected to decrease and thus reduce the amplitude of stick-slip motion. It was also observed that the amplitude of oscillation did not vary with normal load once normal load reached a critical value. This can be explained by the fact that once the maximum real area of contact is achieved at a particular normal load, further increase in normal load does not cause any change in the real area of contact.

3 Conclusions

In the present study, experiments were conducted using an inclined pin-on-plate sliding apparatus to gain an understanding of the effect of surface grinding marks directionality on friction and transfer layer formation of materials with dissimilar hardness. Based on the experimental results, the following conclusions can be drawn:

- The coefficient of friction increases as the grinding angle increases.
- The contribution of plowing friction dominated adhesion in the test conditions.
- The transfer layer depends on the coefficient of friction, which in turn depends on degree of plane strain condition.
- Stick-slip motion depends on the normal load, grinding angle, lubrication, and the material pair.
- The amplitude of stick-slip motion depends on the plowing component of friction.

- In general, the HCP metals showed stick-slip friction phenomenon when compared to FCC metals owing to limited number of slip systems.

References

1. Suh NP (1986) Tribophysics. Prentice-Hall, Englewood Cliffs
2. Rasp W, Wichern CM (2002) Effects of surface-topography directionality and lubrication condition on frictional behaviour during plastic deformation. J Mater Process Technol 125–126:379–386
3. Saha PK, Wilson WRD, Timsit RS (1996) Influence of surface topography on the frictional characteristics of 3104 aluminum alloy sheet. Wear 197(1–2):123–129
4. Bello DO, Walton S (1987) Surface topography and lubrication in sheet metal forming. Tribol Int 20(2):59–65
5. Schedin E (1994) Galling mechanisms in sheet forming operations. Wear 179(1–2):123–128
6. Staph HE, Ku PM, Carper HJ (1973) Effect of surface roughness and surface texture on scuffing. Mech Mach Theory 8:197–208
7. Määttä A, Vuoristo P, Mäntylä T (2001) Friction and adhesion of stainless steel strip against tool steels in unlubricated sliding with high contact load. Tribol Int 34(11):779–786
8. Malayappan S, Narayanasamy R (2004) An experimental analysis of upset forging of aluminium cylindrical billets considering the dissimilar frictional conditions at flat die surfaces. Int J Adv Manuf Technol 23(9–10):636–643
9. Lakshmipathy R, Sagar R (1992) Effect of die surface topography on die-work interfacial friction in open die forging. Int J Mach Tools Manuf 32(5):685–693
10. Menezes PL, Kishore, Kailas SV (2006) Studies on friction and transfer layer using inclined scratch. Tribol Int 39(2):175–183
11. Menezes PL, Kishore, Kailas SV (2006) Studies on friction and transfer layer: role of surface texture. Tribol Lett 24(3):265–273
12. Menezes PL, Kishore, Kailas SV (2006) Influence of surface texture on coefficient of friction and transfer layer formation during sliding of pure magnesium pin on 080 M40 (EN8) steel plate. Wear 261(5–6):578–591
13. Bowden FP, Tabor D (1954) The friction and lubrication of solids. Clarendon, Oxford
14. Menezes PL, Kishore KSV (2006) Effect of roughness parameter and grinding angle on coefficient of friction when sliding of Al–Mg alloy over EN8 steel. ASME J Tribol 128(4):697–704
15. Lovell MR, Deng Z (1999) Experimental investigation of sliding friction between hard and deformable surfaces with application to manufacturing processes. Wear 236(1–2):117–127
16. Challen JM, Oxley PLB (1979) An explanation of the different regimes of friction and wear using asperity deformation models. Wear 53(2):229–235
17. Petryk H (1987) Slip line field solutions for sliding contact. Proc I Mech E, International Conference, Tribology—Friction, Lubrication and Wear 50 years on, London, 2: 987–994
18. Gadelmawla ES, Koura MM, Maksoud TMA, Elewam IM, Soliman HH (2002) Roughness parameters. J Mater Process Technol 123(1):133–145
19. Menezes PL, Kishore, Kailas SV (2008) Effect of surface roughness parameters and surface texture on friction and transfer layer formation in tin–steel tribo-system. J Mater Process Technol 208(1–3):372–382
20. Tanaka K, Kato T, Matsumoto Y (2003) Molecular dynamics simulation of vibrational friction force due to molecular deformation in confined lubricant film. ASME J Tribol 125(3):587–591
21. Gee ML, McGuiggan PM, Israelachvili JN (1990) Liquid to solid like transitions of molecularly thin films under shear. J Chem Phys 93(3):1895–1906
22. Demirel AL, Granick S (1998) Transition from static to kinetic friction in a model lubricated system. J Chem Phys 109(16):6889–6897
23. Ai X, Cheng HS (1996) The effects of surface texture on EHL point contacts. ASME J Tribol 118(1):59–66
24. Buckley DH, Johnson RL (1968) The influence of crystal structure and some properties of hexagonal metals on friction and adhesion. Wear 11(6):405–419
25. Farhat ZN (2001) Contribution of crystallographic texturing to the sliding friction behaviour of FCC and HCP metals. Wear 250(1–12): 401–408